

**Parity-violating asymmetry in nucleon-nucleon scattering at higher energies\***

E. M. Henley and F. R. Krejs†

*Physics Department, University of Washington, Seattle, Washington 98195*

(Received 29 October 1974)

The parity-violating asymmetry of the total cross section for the scattering of longitudinally polarized nucleons from unpolarized proton targets is calculated for energies of 300 MeV-20 GeV. One-pion,  $\rho$ , and  $\omega$  exchanges are included in the computation of the weak force between nucleons. Below energies of roughly 1 GeV, the Watson theorem is adapted to compute the asymmetry. At higher energies an absorptive model is used to take into account hadronic distortion effects.

**I. INTRODUCTION**

In a recent paper, Brown and we<sup>1</sup> reported on a theoretical investigation of the parity-violating (PV) asymmetry in nucleon-nucleon scattering up to about 300 MeV. This limit on the energy was determined by meson threshold effects and the use of a nonrelativistic PV potential. An experiment which searched for this asymmetry in  $pp$  scattering gave a null result,  $(1 \pm 4) \times 10^{-7}$ .<sup>2</sup>

Since experiments are planned at higher energies,<sup>2</sup> both at the Argonne National Laboratory and at the Los Alamos Meson Physics Facility (LAMPF), it is clearly of interest to extend our calculations. The difficulty of carrying out such theoretical predictions stems from a lack of detailed knowledge of both the hadronic and weak interactions. The former of these is required for calculating distortion effects on the weak scattering amplitude as well as for the hadronic matrix element which interferes with the weak one to produce the PV asymmetry.

In this note we report on a simple extension of our previous calculation for the asymmetry<sup>3</sup>  $a$ ,

$$a = \frac{\sigma_+ - \sigma_-}{\sigma_+ + \sigma_-}, \tag{1}$$

of the total nucleon-nucleon scattering cross sections at energies from 300 MeV to 20 GeV. This asymmetry measures the dependence of the total cross section on the helicity of the incident beam. The cross section for positive (negative) helicity is denoted by  $\sigma_+$  ( $\sigma_-$ ). The restriction to total cross section allows us to use the optical theorem

$$\text{Im } \mathfrak{M}_{i,i} = 2k\sqrt{s} \sigma_i, \tag{2}$$

so that we only need to compute the imaginary part of the forward elastic scattering matrix,  $\mathfrak{M}_{i,i}$ , for a given helicity state. In Eq. (2)  $k$  is the magnitude of the c.m. momentum and  $s$  is the invariant c.m. squared energy.

The experimental advantages of detecting parity violation in total-cross-section measurements

have been outlined earlier.<sup>1,4</sup> Because of the short range of the weak interactions, it will probably become advantageous to seek PV effects in the high-momentum-transfer region at very high energies. We briefly discuss such experiments at the end of this work.

**II. THEORY**

In paper I, a PV potential was developed to compute PV effects at energies below 300 MeV. The potential arose from single-boson exchanges, as in Fig. 1(a), and from two-pion exchange. In the present work we omit two-pion-exchange effects, include one-pion-,  $\rho$ -, and  $\omega$ -exchange diagrams, but do not make the nonrelativistic potential approximation. For a given total angular momentum,  $j$ , the PV-admixed state is one which differs in orbital angular momentum by one unit from the "normal" state. The direct inclusion of contributions of PV admixtures (e.g.,  $\frac{1}{2}^-$  states) to the nucleon ground state, Fig. 1(b), requires quark or other models.<sup>5</sup> The model dependence of such effects and those of intermediate  $N^*$  states, as in Fig. 1(c), contributes to the uncertainty of the strength of the effective PV vertex,  $G_{\text{eff}}$ , in Fig. 1(a). We do not explicitly include contributions

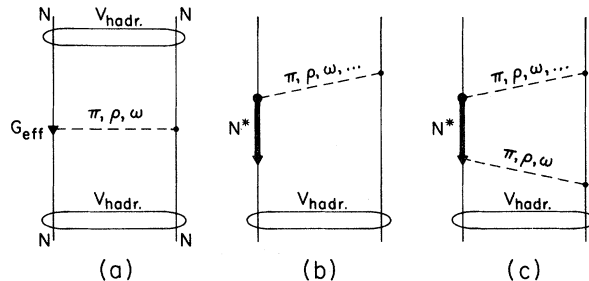


FIG. 1. Some Feynman diagrams for PV nucleon-nucleon elastic scattering. The weak interaction is denoted by a triangle; the oval loop represents a general hadronic interaction.

from diagrams such as those of Figs. 1(b) and 1(c), but assume that they are included in  $G_{\text{eff}}$ .

We use scaling arguments to obtain a further estimate of the magnitude of the PV asymmetry to be expected in high-energy scattering searches.

We split the energy region under consideration into two parts, from 300 MeV to roughly 1 GeV, and from approximately 1 GeV to 20 GeV. As we shall show, the imaginary part of the weak elastic scattering amplitude is proportional to the *real* part of the hadronic elastic scattering amplitude,  $F^{\text{hadr}}$ . In the region below  $\sim 1$  GeV,  $\text{Re } F^{\text{hadr}}$  varies rapidly with energy,<sup>6,7</sup> whereas it is a much more slowly varying function of energy above 1 GeV. To a large extent, it is  $\text{Re } F^{\text{hadr}}$ , rather than the weak interaction, which determines the energy dependence of the asymmetry  $a$ .

If we write the matrix  $\mathfrak{M}$ , Eq. (2), as

$$\mathfrak{M} = M + m, \quad (3)$$

where  $M$  is the hadronic PC (parity conserving) scattering amplitude and  $m$  is the PV matrix, then

$$B_{+,+,+}^{\rho}(\theta) = -16f_{\rho}g_{\rho N}k \left( M + \frac{k^2}{E+M} \right) \left[ \frac{(1+\mu_V)\sin^2(\frac{1}{2}\theta) + \cos^2(\frac{1}{2}\theta)}{m_{\rho}^2 + 4k^2\sin^2(\frac{1}{2}\theta)} + \frac{(1+\mu_V)\cos^2(\frac{1}{2}\theta) + \sin^2(\frac{1}{2}\theta)}{m_{\rho}^2 + 4k^2\cos^2(\frac{1}{2}\theta)} \right], \quad (6)$$

$$B_{+,-,+}^{\rho}(\theta) = 0,$$

where  $\theta$  is the c.m. scattering angle. For  $\omega$  exchange, we obtain the same form, except that  $\mu_V = 0$ , and  $f_{\rho}g_{\rho N}$  is replaced by  $f_{\omega}g_{\omega N}$ . Similar expressions are obtained for the isospin-zero Born-approximation matrix elements, except that the expectation value of  $\vec{\tau}_1 \cdot \vec{\tau}_2 = -3$  in this state. For the  $\pi$  matrix, only  $\pi^{\pm}$  exchange occurs. There is thus no one-pion contribution to the  $pp$  weak matrix element and only an exchange contribution for neutron-proton scattering,  $np \rightarrow pn$ . The charge-exchange (c.e.) cross section at  $180^{\circ}$  contributes to the elastic (el.) forward scattering, so that

$$B_{\lambda_3\lambda_4,\lambda_1\lambda_2}^{\pi,\text{el.}}(\theta) = B_{\lambda_4\lambda_3,\lambda_1\lambda_2}^{\pi,\text{c.e.}}(\pi-\theta),$$

$$B_{+,-,+}^{\pi,\text{el.}}(0^{\circ}) = B_{-,-,+}^{\pi,\text{c.e.}}(180^{\circ}),$$

$$B_{-,-,+}^{\pi,\text{c.e.}}(\theta) = 8\sqrt{2}f_{\pi}g_{\pi N}k \left( M + \frac{k^2}{E+M} \right) \times \frac{\cos^2(\frac{1}{2}\theta)}{4k^2\cos^2(\frac{1}{2}\theta) + \mu^2}, \quad (7)$$

$$B_{+,+,+}^{\pi,\text{c.e.}} = B_{-,-,+}^{\pi,\text{c.e.}} = 0.$$

Similar considerations hold for  $\rho^{\pm}$  exchange in Eq. (6). Although we have given the Born-approxima-

$$M_{\lambda_1\lambda_2,\lambda_3\lambda_4} = M_{-\lambda_1-\lambda_2,-\lambda_3-\lambda_4}, \quad (4)$$

$$m_{\lambda_1\lambda_2,\lambda_3\lambda_4} = -m_{-\lambda_1-\lambda_2,-\lambda_3-\lambda_4},$$

and

$$a = \frac{\sigma_+ - \sigma_-}{\sigma_+ + \sigma_-} = \frac{\text{Im}(m_{+,+,+} + m_{+,-,+})}{\text{Im}(M_{+,+,+} + M_{+,-,+})} = \frac{\text{Im}(m_{+,+,+} + m_{+,-,+})}{4k\sqrt{s}\sigma}, \quad (5)$$

where  $\sigma$  is the spin-averaged total cross section,  $\sigma = \frac{1}{2}(\sigma_+ + \sigma_-)$ . For this cross section, we use experimental data.<sup>6</sup> For the weak matrix element,  $m$ , we use only one-boson-exchange interactions. We include<sup>1</sup>  $\rho$ ,  $\omega$  exchanges for which we assume  $\Delta I = 0$  and  $\pi^{\pm}$  exchange with  $\Delta I = 1$ , where  $\Delta I$  is the change of isospin carried by the weak interaction. In Born approximation,  $m \rightarrow B$ , the helicity projected amplitudes for  $pp$  scattering, for instance, are

tion matrix elements, because we shall make use of them later on, it is actually the distorted-wave (DW) matrix

$$m = \langle \psi^- | H_{\text{PV}} | \psi^+ \rangle \quad (8)$$

which is required in order to take hadronic distortion effects into account.

#### A. $0.3 \lesssim T \lesssim 1$ GeV

In the energy region bounded from above by 1 GeV, it is, in principle, feasible to continue to use the DWBA (distorted-wave Born approximation) method employed at energies below 300 MeV. However, as meson production and relativistic effects increase in importance, the use of the Schrödinger equation and a potential become suspect. It is, however, also difficult to use the absorption model (Sec. II B) to compute distortion effects in this energy region because (a) the real part of the forward scattering amplitude varies rapidly with energy and (b) the elastic differential cross section decreases slowly with increasing momentum transfer so that spatial symmetry considerations become awkward to manage. Despite these difficulties we have used the model to check

the approximate phase-shift method described next.

Phase-shift analyses have been carried out at several energies<sup>8</sup> between 300 MeV and 1 GeV. We shall extend<sup>9</sup> the Watson theorem<sup>10</sup> to evaluate the phase of the weak matrix element, Eq. (8). For the magnitude of the matrix element, we use the Born approximation for all angular momentum states other than those which require an orbital angular momentum zero phase. For  $l=0$  the short-range repulsive core between nucleons reduces the magnitude of any short-range PV matrix.<sup>11</sup> For those PV  $\rho$ - and  $\omega$ -exchange matrix elements which mix orbital angular momenta 0 and 1 ( $j=0, I=1$  and  $j=1, I=0$ ), we assume that the short-range repulsion gives rise to a reduction of the magnitude of the Born-approximation matrix element by a factor of 5. This somewhat arbitrary factor is in line with that suggested by Gari and others<sup>11</sup> for the short-range correlations introduced by the repulsion between nucleons. For the PV pion-exchange matrix element no reduction factor was introduced since this interaction has a considerably larger range.

If it were not for the tensor force, which mixes orbital angular momentum states  $l=j+1$  and  $l=j-1$ , we could use a straightforward application<sup>9</sup> of the Watson theorem to determine the phase of the weak PV elastic scattering matrix element. That is, for a given angular momentum  $j$ , unitarity of the  $S$  matrix completely determines the phase of the off-diagonal PV matrix. Owing to the presence of the tensor force, it is necessary to generalize the Watson theorem. In the representation where  $S_{I=j-1}$  and  $S_{I=j+1}$  are (decoupled) diagonal, this generalization is readily accomplished and we obtain

$$S_j = \begin{pmatrix} e^{2i\delta_-} & i\epsilon e^{i(\delta_+ + \delta_-)} & 0 \\ i\epsilon e^{i(\delta_+ + \delta_-)} & e^{2i\delta} & i\epsilon' e^{i(\delta_+ + \delta_+)} \\ 0 & i\epsilon' e^{i(\delta_+ + \delta_+)} & e^{2i\delta_+} \end{pmatrix}, \quad (9)$$

where  $\delta_-$ ,  $\delta$ ,  $\delta_+$  are the phase shifts for scattering in the states  $l=j-1, j, j+1$ , respectively, and  $\epsilon, \epsilon'$  are the magnitudes of the PV matrix elements which connect the states  $l=j, j-1$  and  $l=j, j+1$ , respectively. Thus the imaginary part of the forward scattering amplitude is

$$\text{Im} f_j = \epsilon_j \text{Im} e^{i(\delta_+ + \delta_-)} + \epsilon'_j \text{Im} e^{i(\delta_+ + \delta_+)}, \quad (10)$$

where the phases are generally complex. For the cases of no tensor-force mixing, the  $S_j$  matrix is a  $2 \times 2$  matrix. This corresponds to  $\epsilon_j$  or  $\epsilon'_j = 0$  in Eqs. (9) and (10). For the analyses carried out at 425, 630, and 970 MeV, the real and imaginary parts of the phase shifts employed by us are listed in Table I. We assume that the magnitude of the

PV matrix elements  $\epsilon_j$  and  $\epsilon'_j$  are given by the angular momentum projections of the Born-approximation matrix elements, Eqs. (6) and (7), reduced by  $\exp[-\text{Im}(\delta + \delta_-)]$  or  $\exp[-\text{Im}(\delta + \delta_+)]$ , whichever applies. This factor is in addition to that introduced by short-range correlation effects, described earlier, which reduces the asymmetry by roughly a factor of 2-4 at the energies considered. With these reductions, the asymmetry computed from the extended Watson theorem matches well the asymmetry computed from distorted waves, Eq. (8), at 300 MeV.<sup>1</sup> Asymmetries were computed for  $g_\omega f_\omega = \pm \sqrt{2} g_\rho f_\rho$ .

### B. $0.85 \leq T \leq 20$ GeV

For kinetic energies above approximately 1 GeV we use the Gottfried-Jackson absorption model<sup>12</sup> to calculate the distorted-wave weak matrix element, Eq. (8). Even here, however, the parameters required for computing the hadronic distortion are not free of ambiguities. The weak matrix can be written as

$$m = 2\pi \int_0^\infty b db J_0(qb) B(b) e^{i\chi(b)}, \quad (11)$$

where  $\vec{q} = \vec{k} - \vec{k}'$  is the momentum transfer,  $b = l/k$  is the impact parameter,  $B(b)$  is the Born-approx-

TABLE I. Phase shifts used for calculating the distortion effects due to the hadronic interaction (Ref. 4). The real parts are listed in degrees and  $\exp(-\text{Im}\delta)$  is given in parentheses when this factor differs from 1. Only isospin  $I=1$  phases are available at 970 MeV. The diagonal phases are given for cases of tensor force mixing.

$T$	425 MeV	630 MeV	970 MeV
$^1S_0$	-19.4	-19.8	-50.8 (0.85)
$^1P_1$	-39.4	-27.3	
$^1D_2$	10.9 (0.95)	9.26 (0.82)	16.0 (0.62)
$^1F_3$	-6.0	-6.4	
$^1G_4$	1.4	5.5	4.5 (0.96)
$^1H_5$	-2.2	-6.2	
$^3S_1$	3.11	-8.3	
$^3P_0$	-18.2	-20.7	-65.9
$^3P_1$	-34.6	-30.0	-48.6 (0.89)
$^3P_2$	17.3	35.1 (0.83)	23.4 (0.86)
$^3D_1$	-36.4	-29.6	
$^3D_2$	8.7	22.5	
$^3D_3$	9.0	-8.9	
$^3F_2$	0.8	-4.5 (0.83)	-4.6 (0.72)
$^3F_3$	-3.7	0.69 (0.82)	-7.7 (0.85)
$^3F_4$	3.3	3.7	6.5 (0.99)
$^3G_3$	9.1	-6.1	
$^3G_4$	0.4	-6.0	
$^3G_5$	-1.5	-7.0	
$^3H_4$	0.08	-2.2	1.1 (0.99)
$^3H_5$	-2.1	-3.2	-2.0 (0.98)

imation matrix for impact parameter  $b$ , and  $\chi$  is the hadronic distorting phase. The phase factor  $\chi(b)$  is found from the elastic scattering amplitude  $F(q)$  by

$$e^{i\chi(b)} \approx 1 + \frac{i}{k} \int_0^\infty q dq F(q) J_0(qb). \quad (12)$$

The imaginary part of  $m$ ,  $\text{Im } m$ , is thus proportional to  $\text{Im } e^{i\chi(b)}$ , which depends on the *real* part of the scattering amplitude  $F(q)$ . Only  $\text{Re } F(0)$  is known experimentally and a further assumption for the  $q$  dependence of  $F(q)$  is required to find  $\text{Im } e^{i\chi(b)}$ . We have used three models.

(1) The simplest assumption is

$$\begin{aligned} \text{Re } F(q) &= \alpha \text{Im } F(q) \\ &= \alpha \text{Im } F(0) e^{-\gamma q^2/2}, \end{aligned} \quad (13)$$

where  $\gamma$  is the slope parameter for  $d\sigma_{\text{el.}}/dq^2$  and  $\alpha = \text{Re } F(0)/\text{Im } F(0)$ . Both of these parameters are known from experiments.<sup>6</sup>

(2) Although assumption (1) is simple, it is not realistic. From Eq. (13) we expect that  $\text{Re } e^{i\chi(b)}$ ,

$$\text{Re } e^{i\chi(b)} = 1 - \frac{1}{k} \int_0^\infty q dq \text{Im } F(q) J_0(qb), \quad (14)$$

is close to unity for small impact parameter  $b$  and falls off to zero in a region  $b \gtrsim 1$  fm, the effective interaction radius. On the other hand, we expect  $\text{Im } e^{i\chi(b)}$ ,

$$\text{Im } e^{i\chi(b)} = \frac{1}{k} \int_0^\infty q dq \text{Re } F(q) J_0(qb), \quad (15)$$

to be zero for both small and large  $b$  and to be peaked in the surface region. It thus seems more reasonable to assume that

$$\text{Im } e^{i\chi(b)} = \beta d[\text{Re } e^{i\chi(b)}] / db. \quad (16)$$

The constant of proportionality  $\beta$  is determined by  $\alpha$ , and  $\text{Re } e^{i\chi(b)}$  is found from Eq. (14), with  $\text{Im } F(q) = \text{Im } F(0) e^{-\gamma q^2/2}$ .

(3) Lastly, we note that Cheng, Chu, and Hendry<sup>3</sup> have managed a good several-parameter fit of  $p$ - $p$  scattering data, including polarization with

$$\text{Im } e^{i\chi(b)} = \frac{f_1}{1 + e^{f_2(b-f_3)}}, \quad (17)$$

where  $f_1, f_2, f_3$  are parameters given in Ref. 13. We have also used this model to obtain  $\text{Im } e^{i\chi(b)}$ .

In all three cases we assume that the hadronic spin-flip amplitudes are negligible, i.e., that the hadronic elastic scattering amplitudes are spin- and isospin-independent,

$$F_{++,+}^{\text{had}} = F_{+,-,+}^{\text{had}}.$$

The validity of this assumption improves with increasing energy. Nevertheless, we have used the

absorption model to calculate the PV asymmetry at a laboratory kinetic energy of 865 MeV in order to overlap with the lower-energy computations. In addition we have computed the asymmetry at kinetic energies of 7.2, 11.6, and 18.7 GeV.

### III. RESULTS AND DISCUSSION

The results of the calculation outlined in Sec. II are shown in Figs. 2-4 for  $p$ - $p$  and  $n$ - $p$  scattering with  $f_\rho g_\rho = 4 \times 10^{-6}$ , and  $f_\pi = 4.3 \times 10^{-8}$ .<sup>1</sup> Since the relative sign and magnitude of  $f_\omega g_\omega$  and  $g_\rho f_\rho$  are unknown,<sup>1</sup> we have computed the asymmetry for  $f_\omega g_\omega = \pm \sqrt{2} f_\rho g_\rho$ . It is difficult to assign an error to our ignorance of the weak forces between hadrons; the error bars in Figs. 2-4 reflect our lack of knowledge of the hadronic interaction. At lower energies, this error is caused primarily by the uncertainty of the behavior of the nuclear force at distances  $\lesssim 0.5$  fm and by our crude way of taking the short-range repulsion into account. At higher energies the error bar reflects the model dependence for the real part of the elastic scattering amplitude. Even the ratio  $\text{Re } F(0)/\text{Im } F(0) \equiv \alpha$  is poorly determined at energies close to 1 GeV (Refs. 6, 7); hence the large error bars at  $T \approx 900$  MeV. We used  $\alpha = -0.2$  at this energy and  $-0.3$  at all energies above 1 GeV.

The reduction of the magnitude of the asymmetry with increasing energy is caused by the decrease in the real part of the hadronic scattering amplitude, and by the nucleon form factor as reflected in the weak force. The change of sign in  $a$  at  $T = 1-5$  GeV for  $f_\omega g_\omega = -\sqrt{2} f_\rho g_\rho$  is related to the change of sign of  $\alpha$ . Physically, the incident nucleon wave packet is damped considerably by

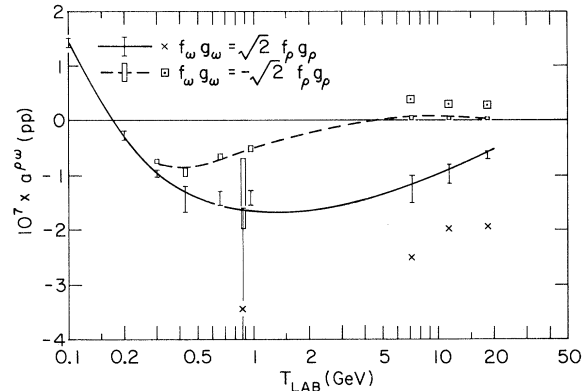


FIG. 2. PV asymmetry due to  $\rho$ - $\omega$  exchanges in total  $p$ - $p$  ( $n$ - $n$ ) cross section as a function of laboratory kinetic energy. The error bars indicate the range of results obtained for various strong-interaction models. The crosses and dotted squares are the values obtained for the model described in Sec. II B, assumption (2). The curves are drawn to guide the reader's eyes.

hadronic effects before it reaches the weak-interaction region of range  $\sim m_\rho^{-1}$ .

At high energies where the hadronic distortion effects are smoothly varying functions of energy and impact parameter, we find  $a^{\rho\omega} \propto (g_\omega + g_\rho)$ . Thus, as seen in Fig. 3, the ratio of the asymmetry ( $a_+$ ) in  $p$ - $p$  scattering for  $f_\omega g_\omega = +\sqrt{2} f_\rho g_\rho$  is

$$\frac{a_+^{\rho\omega}(pp)}{a_-^{\rho\omega}(pp)} \approx \frac{|f_\omega g_\omega| + |f_\rho g_\rho|}{-|f_\omega g_\omega| + |f_\rho g_\rho|} \approx -\frac{2.4}{0.4} \approx -6. \quad (18)$$

For  $n$ - $p$  scattering the contribution of pion ( $\pi^\pm$ ) exchange to the PV asymmetry is shown in Fig. 4 for the Cabibbo value<sup>1</sup> of  $f_\pi = 4.3 \times 10^{-8}$  and for  $g_\pi^2/4\pi = 14.4$ . With this value of  $f_\pi$ , the effect of pion exchange is negligible at all energies and decreases rapidly as the energy increases. Recent gauge theories of weak (and electromagnetic) interactions predict<sup>14</sup> that  $f_\pi$  may be 20–50 times larger than the Cabibbo value. Even such a large increase of  $f_\pi$  does not make the pion contribution comparable to that from  $\rho$  and  $\omega$  exchanges above 1 GeV. The reason for this feature and for the decrease of the pion contribution to the asymmetry with increasing energy is that only charged pions can be exchanged. The weak PV pion force is thus of a purely charge-exchange character, and hence decreases rapidly with increasing energy. The same conclusion is valid for  $\rho^\pm$  exchanges. It follows that only  $\rho^0$  and  $\omega^0$  exchanges contribute to the PV matrix at high energies. Since the hadronic total cross sections for  $p$ - $p$  and  $n$ - $p$  scattering are comparable at high energies, we find

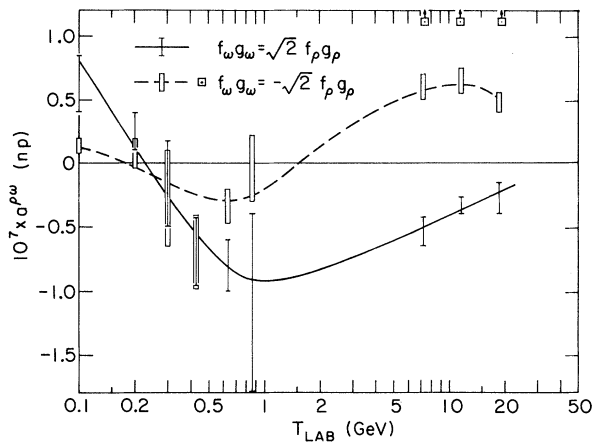


FIG. 3. PV asymmetry due to  $\rho$ - $\omega$  exchanges in total  $n$ - $p$  cross section. See Fig. 2 for legend. The asymmetry for the model of Sec. II B, assumption (2), with  $f_\omega g_\omega = \sqrt{2} f_\rho g_\rho$  lies within the error bars, whereas for  $f_\omega g_\omega = -\sqrt{2} f_\rho g_\rho$  the asymmetry at energies above 5 GeV is  $\sim 2 \times 10^{-7}$  and is indicated by arrows in the figure.

$$\frac{a(np)}{a(pp)} \approx \frac{g_\omega f_\omega - g_\rho f_\rho}{g_\omega f_\omega + g_\rho f_\rho} \approx \begin{cases} \frac{1}{6} & \text{for } g_\omega f_\omega = \sqrt{2} g_\rho f_\rho, \\ 6 & \text{for } g_\omega f_\omega = -\sqrt{2} g_\rho f_\rho. \end{cases} \quad (19)$$

The ratio of the asymmetry in  $n$ - $p$  to  $p$ - $p$  scattering is thus sensitive to the relative sign of  $g_\omega f_\omega/g_\rho f_\rho$ .

The asymmetries plotted in Figs. 2–4 remain small at all energies considered here. Scaling arguments would lead one to expect that the asymmetry increases with energy as  $\sqrt{s}$ . In this case

$$\sigma_{\text{weak}} \approx G^2 s$$

and

$$\begin{aligned} a &\approx \left( \frac{\sigma_{\text{weak}}}{\sigma} \right)^{1/2} \\ &\approx \frac{G\sqrt{s}}{(40mb)^{1/2}} \\ &\approx 10^{-5} \left( \frac{s \text{ (GeV}^2\text{)}}{40} \right)^{1/2}, \end{aligned} \quad (20)$$

where  $s \approx 40 \text{ GeV}^2$  corresponds to a laboratory nucleon of energy  $\approx 20 \text{ GeV}$ . We believe that the

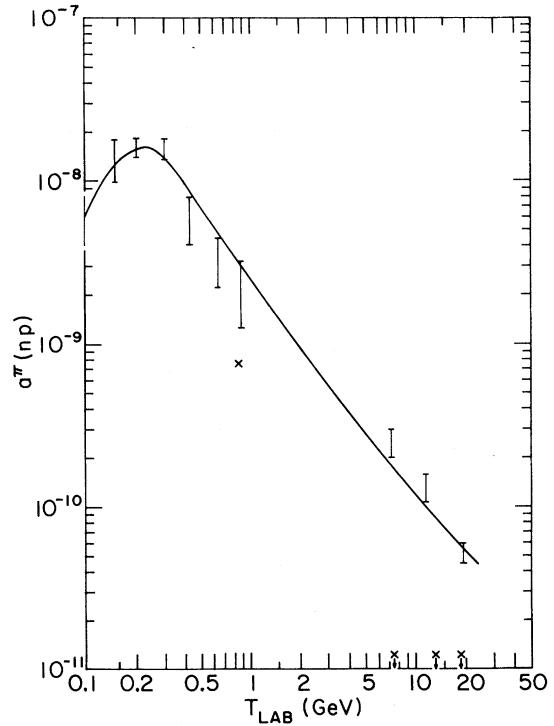


FIG. 4. PV asymmetry due to  $\pi^\pm$  exchanges in total  $n$ - $p$  cross section. See Fig. 2 for legend. The asymmetry for the model of Sec. II B, assumption (2), is found to be smaller by more than one order of magnitude above 5 GeV and is indicated by arrows in the figure.

scaling value for  $a$  is an upper limit in that absorptive effects for  $\sigma_{\text{weak}}$  are omitted; stated another way, Eq. (20) assumes that the weak forward elastic scattering amplitude is purely imaginary. The asymmetry computed by us does not increase as  $\sqrt{s}$  because hadronic absorptive effects increase with energy and reduce the amplitude of the incident wave which reaches the short-range weak interaction. In the absorption model this effect is felt through the exponential damping introduced by  $\exp[i\chi(b)]$  in Eq. (11).

Finally, we want to indicate that total-cross-section measurements may not be the best way to seek PV effects at high energies. Since the weak interactions are due to short-range forces, their effects should become more pronounced at large momentum transfers. Furthermore, hadronic cross sections decrease sharply at large momentum transfers. Experiments and some theories indicate that at a fixed scattering angle and  $k/\sqrt{s}$ , we can expect inclusive reactions such as  $pp \rightarrow p + X$ ,  $p\bar{p} \rightarrow \pi + X$ ,  $\pi p \rightarrow \pi + X$  to have cross sections (measured in  $\text{GeV}^{-2}$ ) (Ref. 15)

$$\frac{E d\sigma_h}{d^3p} \sim \frac{1}{p_\perp^8}.$$

For weak processes, simple scaling arguments give

$$\frac{E d\sigma_{\text{weak}}}{d^3p} \sim G^2.$$

In the gauge theories of weak interactions, the same dependence is obtained and the constant  $G$  is the same [ $G \approx \alpha / (2\sqrt{2} m_W^2)$ ] as long as  $q^2 \ll m_W^2$ .

The interference of the weak and hadronic amplitudes, divided by the hadronic cross section, i.e., the ratio of the weak to strong amplitudes, becomes unity at  $p_\perp^4 \approx G \approx 1$  or  $p_\perp \sim 17$  GeV. Such effects should certainly be detectable, if they are present with this strength. Possible experiments include the use of longitudinally polarized beams and a search for the inclusive-cross-section dependence at fixed  $\theta$  on the direction of the incident beam's longitudinal spin. The interference of weak and strong amplitudes can also be sought with unpolarized beams. For instance, one can look for the inclusive production of  $\Lambda^0$  at large momentum transfers.<sup>16</sup> The characteristic longitudinal polarization, which would arise from an interference of strong and weak amplitudes can be detected from an analysis of the decays of the  $\Lambda^0$ . One may also search for the production of  $\rho$  mesons which are polarized in the scattering plane. Their decays serve to analyze this polarization; e.g., one searches for an expectation

$$\sum_f \langle \vec{J} \cdot \vec{p}_i \rangle \langle \vec{J} \cdot \vec{p}_\rho \times \vec{p}_\pi \rangle - \langle \vec{p}_i \cdot \vec{p}_\rho \times \vec{p}_\pi \rangle,$$

where  $\vec{p}_i$  is the incident momentum,  $\vec{p}_\rho$  that of the  $\rho$ , and  $\vec{p}_\pi$  that of a decay pion.

#### ACKNOWLEDGMENTS

The authors thank Dr. J. D. Bowman, Dr. R. N. Cahn, Dr. H. Frauenfelder, Dr. C. F. Hwang, Dr. L. Lederman, Dr. J. L. McKibben, Dr. R. E. Mischke, and Dr. D. E. Nagle for helpful discussions and communications.

\*Work supported in part by the U. S. Atomic Energy Commission.

†Present address: Physics Dept., University of Pennsylvania, Philadelphia, Penna. 19174.

<sup>1</sup>V. Brown, E. M. Henley, and F. R. Krejs, Phys. Rev. C **9**, 935 (1974), referred to as paper I.

<sup>2</sup>J. M. Potter *et al.*, Phys. Rev. Lett. **33**, 1307 (1974), and private communication.

<sup>3</sup>Note that the asymmetry  $a$ , as defined by Eq. (1), is  $\frac{1}{2}A$ , the asymmetry as defined in Ref. 1. The present definition is the preferred one.

<sup>4</sup>M. Simonius, Phys. Lett. **41B**, 415 (1972); E. M. Henley, in *Few Particle Problems in the Nuclear Interactions*, edited by I. Slaus, S. A. Moszkowski, R. P. Haddock, and W. J. H. Van Oers (North-Holland, Amsterdam, 1972), p. 222.

<sup>5</sup>See, e.g., E. M. Henley, T. E. Keliher, W. J. Pardee, and D. U. L. Yu, Phys. Rev. D **8**, 1503 (1973).

<sup>6</sup>Particle Data Group, UCRL Report No. UCRL-20000 NN, 1970 (unpublished).

<sup>7</sup>I. V. Amirkhanov *et al.*, in *High Energy Physics and Nuclear Structure*, edited by G. Tibell (North-Holland, Amsterdam, 1974), p. 47; O. V. Dumbrais, Yad. Fiz. **13**, 1096 (1971) [Sov. J. Nucl. Phys. **13**, 626 (1971)].

<sup>8</sup>For a summary, see N. Hoshizaki, Fiz. Elem. Chastits At. Yad. **4**, 79 (1973) [Sov. J. Part. Nucl. **4**, 39 (1973)].

<sup>9</sup>E. M. Henley and B. A. Jacobsohn, Phys. Rev. **113**, 225 (1959); S. Fubini and J. D. Walecka, Phys. Rev. **116**, 194 (1959); E. M. Henley, T. E. Keliher, W. J. Pardee, and D. U. L. Yu, Phys. Rev. D **9**, 755 (1974).

<sup>10</sup>K. M. Watson, Phys. Rev. **95**, 228 (1954).

<sup>11</sup>M. Gari, Phys. Rep. **6C**, 318 (1973).

<sup>12</sup>K. Gottfried and J. D. Jackson, Nuovo Cimento **34**, 735 (1964).

<sup>13</sup>T. Cheng, S. Chu, and A. Hendry, Phys. Rev. D **7**, 86 (1973).

<sup>14</sup>See, e.g., M. K. Gaillard and B. W. Lee, Phys. Rev. Lett. **33**, 108 (1973); D. Bailin, A. Love, D. V. Nanopoulos, and G. G. Ross, Nucl. Phys. **B59**, 177 (1973).

<sup>15</sup>J. F. Gunion, S. J. Brodsky, and R. Blankenbecler, Phys. Rev. D **6**, 2652 (1972); S. F. Brodsky, in *High Energy Collisions—1973*, proceedings of the fifth International Conference on High Energy Collisions, Stony Brook, 1973, edited by C. Quigg (A.I.P., New York, 1973).

<sup>16</sup>N. N. Nikolaev, Yad. Fiz. **17**, 119 (1973) [Sov. J. Nucl. Phys. **17**, 62 (1973)].